ACS APPLIED ELECTRONIC MATERIALS

pubs.acs.org/acsaelm Article

Temporary Tattoo Approach for a Transferable Printed Organic Photodiode

Bernhard Burtscher, Guenther Leising, and Francesco Greco*

Cite This: ACS Appl. Electron. Mater. 2021, 3, 2652−2660 Read Online

ACCESS | Metrics & More | Article Recommendations | Supporting Information

ABSTRACT: Generation of ultrathin, transferable, and imperceptible electronic devices [e.g., organic photodiode (OPD)] for multiple applications, such as personalized health monitors and wearables, is emerging due to the continuous development of materials and manufacturing processes. For such devices, the choice of a suitable substrate is of utmost importance. A water decal transfer from a temporary tattoo paper is adopted here as a substrate for ultrathin and conformable organic components because of easy and reliable transfer of a ≈600 nm robust and transparent polymer nanofilm of ethyl cellulose. Strategies for the fabrication of a transferable OPD on a temporary tattoo are investigated. A device with an overall thickness <1 μm and its performance after transfer are demonstrated. Then, efforts are put into fabricating an OPD by inkjet printing with a water-soluble active layer consisting of polythiophene and fullerene derivatives to aid cost- and material-efficient, large-scale production possibilities. Additionally, a second semi-transparent electrode made of printed aluminum-doped zinc oxide and silver nanowires is used to allow usage from both sides to enhance the application potential. Both OPD examples presented here need improvement of the device performance but permitted us to highlight the versatility and application potential of temporary tattoos for transferable components. Target surfaces for the final application after transfer include artificial (flat and smooth, e.g., glass, or even complex and rough, e.g., concrete, paper, and so forth) as well as natural ones.

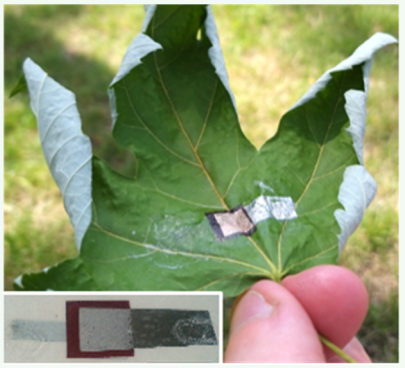

KEYWORDS: *temporary tattoo, organic photodiode, printed electronics, conformable electronics, transferable*

INTRODUCTION

Wearable electronics[1] and lab-on-skin devices[2] have gained a lot of interest over the last few years. These epidermal sensors can obtain information from the skin about hydration and temperature and can monitor electrophysiological signals[3] or the oxygen level in the blood, to name a few. In contrast to more cumbersome state-of-the-art devices, these thin and soft epidermal devices can conformably adhere to the skin. Skin, as an example for a complex surface, has topographical features with a typical lateral size of hundreds of micrometers (μm) and heights of tens of μm.[4] Because of their conformability, these epidermal devices are almost imperceptible when worn, thus offering great promise for future personal monitoring even long-term. Current challenges include, among others, the integration of multiple functionalities and subsystems into an epidermal device, such as power supply and data communication, as well as adopting strategies for large-scale production.[1,2] Moreover, the target of transferable, conformable devices is not just limited to skin applications: more and more target surfaces are in principle addressable, enabling unprecedented applications. One very promising strategy for this type of applications is based on a decal-transfer temporary tattoo paper (TT) as a support for transferable ultrathin electronics. TT has been shown to be of low-cost, imperceptible, conformable, and easy to handle and transfer onto target surfaces.[5] Furthermore, recent examples include tattoo-based edible electronics on foods and drugs,[6] monitoring of crops, and sensing of microclimate and growth with so-called "plant wearables".[7,8] With the right choice of materials, conformal devices can also enable novel directions for "transient electronics"[9−14] and in the development of, for example, transient sensors that can safely degrade in the environment after their use. Materials other than TT have been used for wearable electronics[2,15−17] and some have shown superior stretchability. However, often they are thicker and therefore lose some conformability and are more noticeable when worn, especially over an extended period. Some of these have intrinsic adhesive properties (e.g., polydimethylsiloxane); others need additional glue layers to adhere to the skin or other target substrates. Other approaches utilize different transfer techniques to solve this issue.[18,19] Recently, various approaches to ultraconformable electronics[15] and specific

Received: March 16, 2021
Accepted: June 1, 2021
Published: June 10, 2021

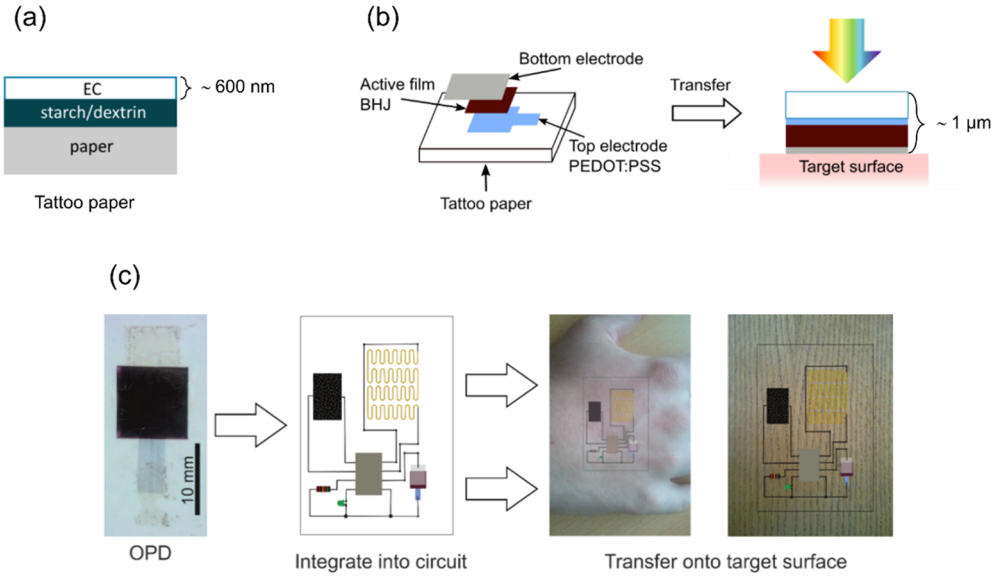

Figure 1. TT and transferability. (a) Layout of a TT with a releasable layer of EC and a sacrificial water-soluble layer of starch/dextrin; (b) stacked scheme structure of the OPD and transfer process; and (c) OPD prototype before transfer (on back-paper) with the possibility to include into a circuit and transfer onto target surfaces.

examples and features of electronics on TT[5] have been reviewed, highlighting the opportunities and challenges.

The first and main requirement for conformable devices is being transferable and conformally adherent onto a target surface while ideally being flexible and stretchable as well. Besides these requirements, additionally, they should be easy to handle and stable (both mechanically and chemically). Thin-polymer materials (<1 μm) show very good conformability to a variety of surfaces, including those having a complex texture.[20] They can provide sufficient electrical insulation and are thus envisioned as optimal substrates for conformable electronics. However, usually such thin free-standing polymer films are not easy to process and handle. An unconventional substrate, which has shown great promise for the development of skin-worn sensors, is decal transfer paper commonly used as temporary tattoos for children.[1,21−23] Such a commercially available skin-friendly substrate combines the required thickness/conformability with very low price and processability. Its use as a substrate for several electronic devices has been studied by some groups with most of the development focusing on skin-contact human biomonitoring[5] but also exploring novel opportunities with other target surfaces.[6,24] A recent example showed the fabrication of an organic light-emitting diode on a TT that was transferred onto a plastic bottle.[25] Whereas these examples have shown the potential of TTs for transferable electronics, the device complexity either remains quite simple, focusing on 2D-layouts,[3,23,24] or needs additional steps during manufacturing (protection[25] or inert annealing[6]). Increasing the device complexity while keeping the fabrication simple is therefore one of the challenges to be tackled. These include fabrication under ambient conditions from economic precursors, new photo-active water-soluble blends, a stacked-layer approach on TTs without a protection layer, and usage of inkjet printing.

One way to address large-scale production of transferable devices could be the use of printing techniques such as inkjet, screen, or gravure printing. Inkjet printing as a non-contact fabrication technique allows for low-cost and resource-friendly production. Moreover, the number of jettable functional available materials is increasing, expanding the spectrum of possible developments. Especially, printable organic materials are of great interest as they concur with the demands for flexibility and sometimes even stretchability.[26] This makes them great candidates for manufactured conformable devices.[15]

In order to build up a complete conformable electronic system on board of a transferable thin substrate, ad-hoc fabrication strategies are needed for several electronic subcomponents, such as organic field-effect transistors[20] and power supply (e.g., fuel cell, batteries, solar cells).[21,24,27,28]

Among various subcomponents, organic photodiodes (OPDs) are quite interesting as they could be used for receiving optical signals for both sensing and communication purposes. For bio-related applications, these have been used in a battery-free, wireless pulse oximeter,[29] creating 2D oxygenation maps[30] or to estimate drowsiness[31] among others. Whereas flexible and stretchable OPDs have been demonstrated,[30,32−34] these have often no direct possibility of transfer and/or only show limited to no conformability. Because of this, discomfort while wearing can occur, which was not observed with TT even after extended times.[3] In addition, their fabrication strategies are often not as versatile and easily upscalable as printing methods. Therefore, TT would be a novel albeit unconventional approach for this issue.

Some attempts to fabricate OPDs onto unconventional substrates have been reported, for example by Lamprecht et al.,[35] who used a newspaper as a substrate. Coating by vapor deposition of Parylene C and Ormocere on paper was required prior to fabricate the OPD, obtaining a suitably smooth and robust substrate. Indeed, the fiber-like nature of paper makes it impossible to directly build up a thin-film device.

Inspired by this example, our study focuses on materials and fabrication strategies for obtaining an OPD based on a polythiophene−fullerene bulk heterojunction (BHJ)[36] onto a commercially available TT. The layout of a commercial TT, the general idea of a transferable OPD, and future ideas to realize full electronic circuits on it are displayed in Figure 1. This approach can allow for easy transfer and adhesion of the

https://doi.org/10.1021/acsaelm.1c00249
ACS Appl. Electron. Mater. 2021, 3, 2652−2660

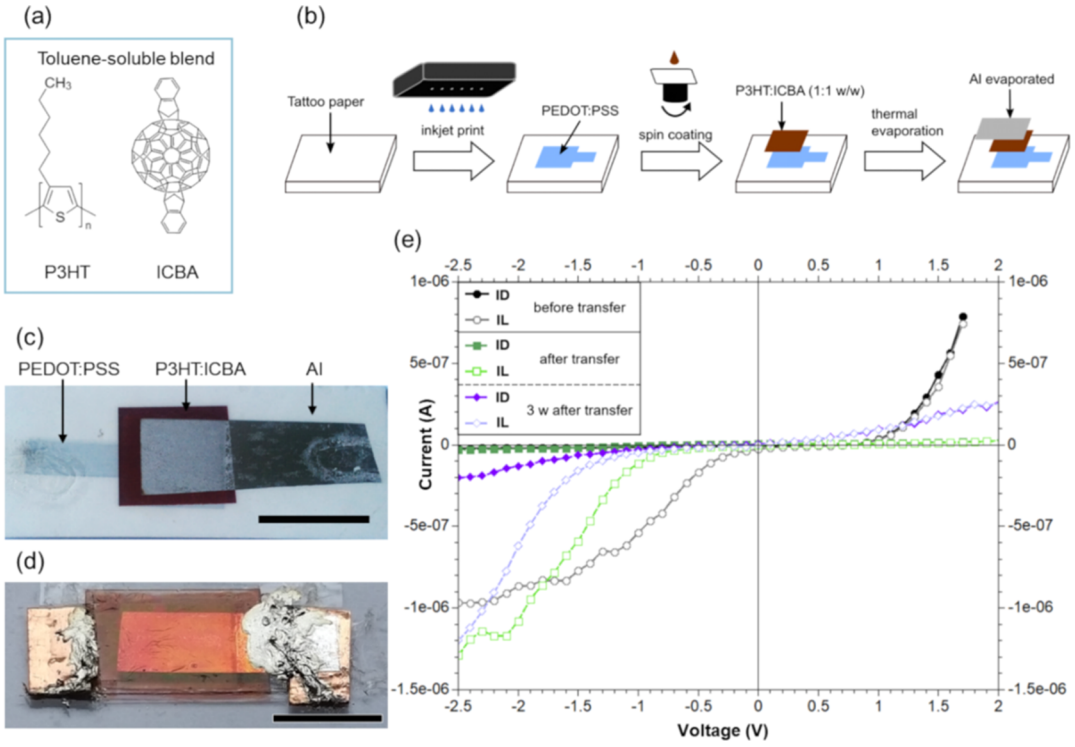

Figure 2. OPD of PEDOT:PSS/P3HT:ICBA(1:1 w/w)/Al. (a) Chemical structure of a toluene blend for an active film; (b) scheme of the fabrication process; (c) image of the OPD before transfer (scale bar: 10 mm); (d) image of the OPD after transfer onto glass with connections repaired with silver epoxy (scale bar: 10 mm); (e) I/V-characteristic curve of an OPD without (ID) and with (IL) an illuminance of (75 700 ± 300) lx. The sample was 6 months old when measured before transfer. It was measured within 48 h after transfer and again 3 weeks after transfer.

device onto target surfaces, including but not only onto skin. Because of the foreseen OPD application, a first question regarded the suitability of TT to act as a transferable substrate; we investigated its transparency in the visible light range, stability against wet or vacuum processing, its thickness, and whether its surface is smooth enough to enable fabrication and operation of an OPD. Therefore, we investigated and tested various strategies for the deposition of electrodes and active organic semiconductor blends for a BHJ. For printing techniques, the wettability of the substrate is important to obtain homogeneous films. It can be improved through plasma treatment of the substrate.[37] While the final goal is to have a full inkjet-printed conformable device, we approached the problem in two steps, providing a more meaningful comparison with the existing literature and a first proof-of concept demonstration for our devices. First, we adapted the fabrication processing of a BHJ with a well-known and studied organic donor−acceptor blend: poly(3-hexylthiophene) (P3HT) and indene-C60 bisadduct (ICBA) (Figure 2a). In this first case, the processing was based on inkjet printing, spin-coating, and a final vacuum-based deposition of a top Al electrode. Afterward, with the aim of providing a fully printed ultrathin and transferable OPD, we investigated the water-soluble organic semiconductors (poly[3-(potassium-4-butanoate)thiophene-2,5-diyl]) (P3P4T) and C60 pyrrolidine trisacid ethyl ester (PyC60) (Figure 3a) as components of a jettable photoactive layer. The processing was all solution-based with all the layers inkjet-printed except for a drop-casted layer of Ag nanowires (Ag NWs) acting as a second transparent electrode. Furthermore, no protection layer is used in our approach although a vertical layout is chosen. Indeed, one drawback of the TT is its limited chemical stability compared to other—more expensive and less easily transferable—polymer substrates, such as polyimide, polyethylene naphthalate, and parylene. This can be circumvented to allow a stacked layout by adding layers,[25] which in turn can affect its conformability.

RESULTS AND DISCUSSION

Substrate(S). The investigation on transferable substrates started with a preliminary screening of different commercially available TTs and a medical polyurethane adhesive recently adopted for skin-mounted sensors.[5,38,39] Among the studied substrates, further details can be found in a recent review,[5] a TTs (namely, the one commercially available as a DIY kit by "The Magic Touch", see the Experimental Section) was found to best match the requirements and, therefore, was chosen as a substrate as already done for other applications.[3,6,22−24] This TT permits the release of a thin ethyl cellulose (EC) film upon wetting with water and dissolution of a sacrificial starch layer (Figure 1a). EC is a robust, biofriendly, and even edible polymer used as an additive in many pharmacological formulations and as a film in skin-contact applications.[40] An optical microscopy image and an atomic force microscopy (AFM) image of the EC film released from a TT are given in the Supporting Information (Figure S1). The released EC film has a thickness of t = (608 ± 52) nm and a roughness of R_a = (13 ± 3) nm, as estimated by means of profilometry and AFM topography imaging.

The obtained values of thickness and R_a are considered suitable for the foreseen conformable electronics applications. These substrate features are indeed crucial in assessing its adoption for conformable electronics. The best conformability to target surfaces and imperceptibility when worn on skin can

https://doi.org/10.1021/acsaelm.1c00249
ACS Appl. Electron. Mater. 2021, 3, 2652−2660

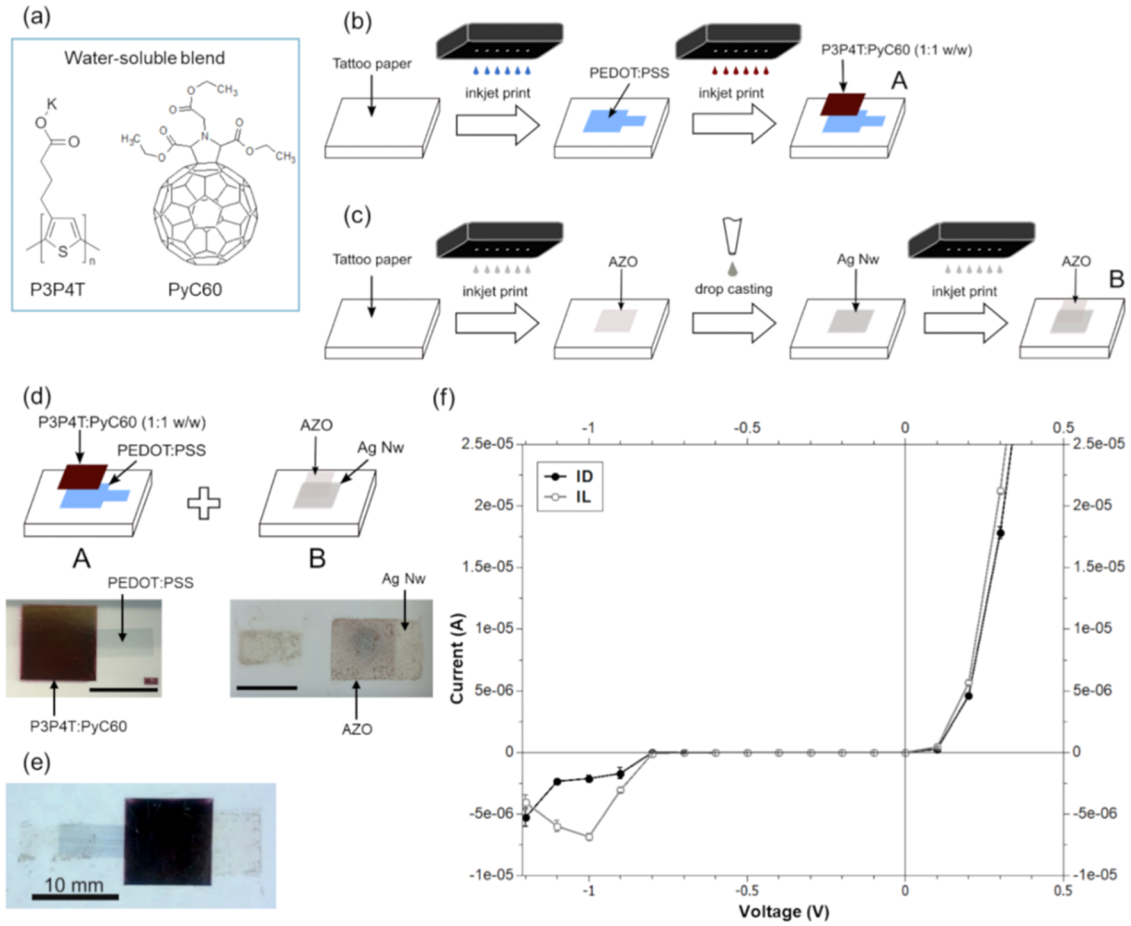

Figure 3. OPD of the PEDOT:PSS/P3P4T:PyC60(1:1 w/w)/AZO electrode. (a) Chemical structure for the water-soluble blend; (b) fabrication steps of part A; (c) fabrication steps of the AZO electrode (part B); (d) structure and images of the two parts before lamination (scale bar: 10 mm); (e) OPD after laminating part A onto part B; (f) I/V-characteristic curve of a 3-month-old OPD without (ID) and with (IL) an illuminance of (75 700 ± 300) lx.

be attained with a thin (sub-μm range) polymer substrate.[41] On the other hand, a low roughness is important for thin-film device patterning since a smooth surface is required to achieve uniform thin-film deposition without pinholes and defects.

The EC film transferred on a glass slide showed very good transparency (>98%) over the full visible-light range as required for a photodiode operating in this range (UV/vis spectrum of EC in Figure S2). Moreover, the compatibility of the TT substrate with toluene was preliminarily tested. Some tens of microliters of the solvent was dispensed on TT, left to dry at room temperature, and then the EC layer was transferred without noticing any difference in release with pristine TT.

Once the transferable substrate was chosen, materials and layouts of OPD were investigated. In any of these layouts, at least one transparent electrode is needed. For the two OPD layouts considered in this study, the first layer to be deposited is therefore the semitransparent top electrode made of PEDOT:PSS, by inkjet printing of a waterborne system. PEDOT:PSS is commonly used as a hole-transporting layer in organic photovoltaic cells and OPDs.[36] Prior to printing an air plasma, activation of the EC surface was necessary to achieve a good wettability and homogeneity. Changing the drop spacing (DSP) settings in the inkjet printing affected the thickness and conductivity of the electrodes (Figure S3). An optimal spacing was thus set at DSP = 35 μm and a two-layer layout was chosen ($t \approx 60$ nm), which resulted in a conductivity of σ = (670 ± 110) S cm^{-1} comparable to literature values.[42]

This satisfactory conductivity was accompanied by good transparency (transmittance >80%) in the visible range of the bilayer EC/PEDOT:PSS (Figure S2).

EC has shown to undergo morphology changes when exposed to temperatures >150 °C,[22] which should be considered when devising fabrication strategies. Depending on the exact composition and addition of plasticizers, EC films were reported to be more or less sensitive to humidity during storage[43] with an average reported moisture absorption (23 °C, 50% RH) of around 2%.[44] From our experience, we observed that devices based on EC films from TT can be stored and remain well attached to the target substrate after 2 years [when stored in a cupboard (Figure S4)]. The functionality and exact specifications of device properties will instead depend on the final application as skin-worn devices and insulating or conducting substrates have different requirements.

For the measurement of EC in the NIR (Figure S5), five layers of EC were collected onto a glass slide and showed a transmittance of >90%. Therefore, temperature increase due to absorption is deemed negligible in the EC layer.

OPD with PEDOT:PSS/P3HT:ICBA/Al. An OPD BHJ with the well-known donor−acceptor organic semiconductors P3HT and ICBA was fabricated on top of a TT. Their

https://doi.org/10.1021/acsaelm.1c00249
ACS Appl. Electron. Mater. 2021, 3, 2652−2660

chemical structures are displayed in Figure 2a, while the layout of this OPD and the fabrication steps are schematized in Figure 2b. Evaporation of Al was chosen for fabricating the bottom electrode, resulting in a device thickness of ∼1 μm with the EC layer. Pictures of such an OPD before and after transfer (onto glass slide) are shown in Figure 2c,d, respectively. The I/V-characteristic curves of a sample were recorded 6 months after fabrication. Measurements were carried out before and after transfer (48 h and 3 weeks) onto a glass slide (Figure 2e). Both ID (dark current, no illumination) and IL (photo-current, during illumination with LED) are shown for comparison for each test. The black and gray curves refer to the same sample still supported on paper before the transfer. Even after 6 months since fabrication, a photodiode behavior could clearly be seen as in forward direction, a current flowed while in reverse bias, the current is enhanced when the photodiode is illuminated. Photosensitivity was retained although it has been affected by aging since it starts only after applying a negative voltage.

The dark and light green curves have been recorded within 48 h after transfer. In the forward direction, the current flow started at a higher voltage than before the transfer. Again, a photodiode behavior is observed, as under reverse bias, one can clearly distinguish between ID and IL. Measuring the same sample 3 weeks later resulted in the purple curves; there an applied negative voltage still allowed for distinguishing between ID and IL although the ID was higher than for the other measurements.

In all three cases, one can distinguish between curves with and without illumination but their behavior slightly differs. Evidently, the curves after transfer in the forward direction showed a lower current. The differences under a negative bias were not much drastic. The higher IL observed (at ∼−2 V) after the transfer (bright green and purple) compared with that before transfer (gray curve) is caused by the fact that before transfer the sample had to be illuminated through the back support-paper, since the use of a reflective Al layer as the bottom electrode prevented a direct illumination through it. Comparison with another OPD with an active layer of P3HT/ICBA (1:1) in toluene and a similar structure, except for an additional ITO and a Ca layer between the active layer and Al, shows good agreement in the dark curve regarding the threshold.[45] A higher annealing temperature (150 °C), the additional ITO and Ca layers, different substrates, and I/V characteristic measurements carried out under a N_2 atmosphere could all be reasons for the difference in behavior under illumination besides the time differences in fabrication and measurements. The I/V-characteristic of the OPD with a logarithmic scale, for better visibility of the on−off ratio, can be seen in Figure S6.

Overall, the obtained results permitted us to assess the suitability of the proposed approach for producing a transferable ultrathin OPD, as confirmed by retaining a functional photodiode behavior after transfer. The behavior of a device measured directly after fabrication is shown in Figure S7, where a clear distinction between ID and IL before and after transfer is possible. After transfer, a comparable on−off ratio ($\sim 10^2$) is attainable, although interestingly ID is reduced for most measured voltages except when more negative than −1.2 V. The device showed an open-circuit voltage of ∼0.46 V compared to 0.58 V[46] in a device with a similar structure from literature. It should be mentioned again that the OPD before transfer had to be illuminated through the TT still supported on paper and therefore comparison to literature should be done with this in mind.

OPD with the PEDOT:PSS/P3P4T:PyC60/AZO Electrode. After testing the feasibility of fabrication and transfer of an OPD with a temporary tattoo approach, some efforts were dedicated to developing a strategy for obtaining a fully printed and more bio-friendly device. To this purpose, water-soluble polythiophene (P3P4T) and fullerene (PyC60) derivatives were utilized. Furthermore, a modification of the layout was introduced by using a second semitransparent electrode, enabling usage from both sides and to enhance application potential. This electrode made of inkjet-printed aluminum-doped zinc oxide (AZO) and drop-casted Ag NWs on EC had a transmittance of >40% in the visible range (Figure S2). The chemical structure of the materials used in the water-based ink [P3P4T:PyC60 (1:1 w/w)] for the photoactive layer is shown in Figure 3a. Good wettability and thus printability could be achieved with this ink after performing an air plasma activation, obtaining a homogeneous layer on both the pristine TT and PEDOT:PSS film, as visible in Figure S8. The annealing temperature was reduced to 90 °C as less homogeneity was observed in the P3P4T:PyC60 layer with higher temperatures.

To fabricate such an OPD, two parts (A and B) were manufactured separately on two different sheets of TT (Figure 3b,c) and then coupled together through lamination (A + B, Figure 3d). Two parts were necessary as the printed photoactive layer is damaged when Ag NWs are directly deposited onto it, due to partial re-dissolution. Moreover, this strategy permitted us to encapsulate the whole OPD in between two layers of insulating EC, thus preventing the direct contact of the electrode and active layer to target surfaces. This can be important in several envisioned applications, especially when biological surfaces are targeted.

Part A is illustrated in Figure 3b where PEDOT:PSS is printed onto TT and then the active film inkjet-printed. A comparison of the UV/vis absorbance of the two donor−acceptor blends used in this study, P3HT:ICBA (1:1 w/w) and P3P4T:PyC60 (1:1 w/w), is given in the Supporting Information (Figure S9). A shift of the maximum absorbance peak position of (49 ± 3) nm is observed in the water-soluble blend with respect to P3HT:ICBA. Figure 3c shows the fabrication scheme of part B on another TT. An electrode obtained by drop-casting of Ag NWs did result in a relatively high sheet resistance (R_S = (160 ± 200) Ω/□) and poor homogeneity. While the use of Ag NWs would, in principle, allow for a better conductivity after annealing (150 °C, 30 min),[47] on TT, this proved to be challenging because of the limited temperature stability of EC.[22,48,49] Indeed, in a previous study on the same TT paper, heating of a sample at 150 °C resulted in partial degradation of surface roughness due to recrystallization upon heating of EC, which could be detrimental for the operation of the OPD.[22] Thus, different processing strategies should be adopted. To this aim, a layer of AZO was first printed before depositing Ag NWs, permitting us to achieve an electrode with a lower sheet resistance (R_S = (12.4 ± 5.1) Ω/□). Therefore, the processing presented here was found as suitable for the obtainment of an electrode without compromising the stability of the underlying layer. More information on this is provided in the Supporting Information (Table S1) as well as SEM images (Figure S10) of Ag NWs on EC. A second AZO film is then printed (five consecutively printed layers) to function as a blocking layer and to help reduce the short-circuit potential. The assembled

https://doi.org/10.1021/acsaelm.1c00249
ACS Appl. Electron. Mater. 2021, 3, 2652−2660

device (A + B) is displayed in Figure 3e. A shift of open-circuit potential upon illumination was observed immediately after fabrication, confirming light-sensitivity. An I/V-characteristic curve taken 3 months after fabrication, ID (gray curve) and IL (black curve), is seen in Figure 3f. The OPD shows a diode behavior with a low dark current for the reverse bias and a current flow in the forward direction. A photoresponse is only noticeable in a small range around −1 V, concurrent with a rise of the dark current. Before that, a differentiation between ID and IL given the uncertainty is not possible. The OPD with a logarithmic scale is shown in Figure S11.

Realizing a transferable OPD only through printing techniques with a second semitransparent electrode was investigated. Although only a weak light response can be shown, some accomplishments were still achieved. First, an OPD could be fabricated with a non-vacuum-based process onto an unconventional, transferable, commercial TT, which with its thickness of ∼600 μm ensures conformability. Second, a novel water-soluble active film inkjet-printable formulation consisting of P3P4T and PyC60 was investigated. The study regarded their printing parameters as well as incorporation into a device structure. A lamination approach with two TT substrates was implemented to include a second semi-transparent electrode in this device structure, composed of a combination of AZO and Ag NWs and to provide an encapsulation of the OPD in between two insulating EC layers. Due to the time between fabrication and measurement, degradation was observed, as it could be expected. Improving the performance of the OPD, either through different additional layers or encapsulation, or trying to minimize the degradation during transfer are all viable options for further investigation. Since other water-soluble polythiophenes with different lengths of side-chain are available, they could be investigated as their properties vary slightly.[50] Since measurements were taken some time after fabrication, a tentative assessment of storability could be done. In the case of OPD with P3HT:ICBA, functionality was maintained even months after fabrication. The same cannot be said about OPDs with a P3P4T:PyC60 structure although encapsulated by EC. Differences in the chemical structure can be responsible for this as well as that EC is permeable to water vapor[51] and therefore not being an ideal encapsulation for protection against water. The extent to which this affects the performance of the device should be evaluated with respect to a particular application since mechanical durability, electrical and temperature insulation, and moisture protection depend not only on the application but also on the target surface.

CONCLUSIONS

In conclusion, it was possible to fabricate an OPD onto a TT with a device thickness of <1 μm to have a transferable device. OPD operation was demonstrated before and after transfer as well as after several months after fabrication. Furthermore, excellent conformability was shown of a TT OPD on a plant leaf (Figure S4a). Stable and conformal adhesion on the leaf surface was retained when the leaf started to dry, shrink, and crumble (Figure S4b). Stable adhesion and no delamination can even endure for more than 1 year with the OPD tattoo acting as a "second skin" on the leaf surface (Figure S4c). Only a weak light response could be accomplished with a fully printed device, which demands further investigations to achieve improvement of photosensibility and to extend the fabrication by printing.

Combining the custom patterning offered by inkjet printing with an easy transfer strategy and the usage of cheap, ultra-light-weight, and mass-produced substrates accompanied with good conformability and storability can provide a boost toward transitioning of OPD tattoo devices to industrialization and adoption in real-life scenarios.

EXPERIMENTAL SECTION

Materials. A TT called "Tattoo Transfer 2.1" from TheMagic-Touch GmbH was used as a substrate.

PJet 700 (PEDOT:PSS) from Heraues (solid content: 0.6−1.2%) was used for printing the top electrode. Therefore, it was filtered with a 0.20 μm cellulose acetate (CA) syringe filter and stored for some hours to get rid of air bubbles before inkjet printing.

AZO ink (H-DZ01015) was stored wrapped in aluminum foil after filtering it with a 0.20 μm PTFE syringe filter. Solvents for this ink (solid content: ≥1−<2.5%) are α-terpineol and *n*-butanol.

Ag NWs (Aldrich: 778095-25ML) with Ø of 120−150 nm and a length of 20−50 μm suspended in 0.5 wt % isopropyl alcohol were used.

Al (Umicore: 0481534) was evaporated through a MED010 from Balzer Union.

P3HT (Rieke Metals: 4002-E) and ICBA (Aldrich: 753955-250MG) were dissolved (1:1 w/w) in toluene (Aldrich: 34866-1L-M) with 15 mg/mL of P3HT/solvent. After stirring for about 24 h at 80 °C, the temperature was reduced to 50 °C and before use filtered with a 0.20 μm PTFE syringe filter.

P3P4T (Rieke Metals: 4021) and PyC60 (Aldrich: 709093-250MG) were dissolved in 18 MΩ water (gained from Sartorius AG: arium mini plus) in a ratio of 1:1 w/w with 10 mg/mL P3P4T/solvent at 80 °C. After 24 h, the temperature was reduced to 50 °C and continuous stirring applied until filtering with a 0.20 μm CA syringe filter into a cartridge. The ink container was wrapped in an aluminum foil during storage.

Fabrication of OPD PEDOT:PSS/P3HT:ICBA/Al. A schematics of fabrication steps is provided in Figure 2b,c. Printing the top electrode (PEDOT:PSS) of (10 × 10) mm^2 plus connection (see Figure 1b,c) was done with a DMP2850 from Fujifilm after treatment with air plasma (Diener electronic Femto) at p = 0.3 mbar and 22 W for 10 s. Two layers of PEDOT:PSS were printed with a DSP of 35 μm; in-between the two printing steps, an IR-treatment at $T \approx 80$ °C for 3 min was carried out with a self-made system consisting of a lamp (Osram HLX Xenophot) that is focused with a mirror onto the printing plate. Afterward, the sample was annealed at T = 120 °C for 10 min.

P3HT:ICBA (1:1 w/w) was spin-coated (CHEMAT technology KW-4A, 60 s, 800 rpm) after masking with Parafilm ((11 × 11) mm^2). After removing the mask, the sample was annealed at T = 120 °C for 10 min. For Al evaporation at $p = 2 \times 10^{-3}$ mbar, a (10 × 15) mm^2 mask with a thread seal tape was used.

Fabrication of the OPD PEDOT:PSS/P3P4T:PyC60/AZO Electrode. The OPD was produced in a two-step process onto two separate TT substrates, which were then coupled through lamination. For part A, first a PEDOT:PSS layer was printed according to the procedure described above for the PEDOT:PSS/P3HT:ICBA/Al OPD. Printing of P3P4T:PyC60 (1:1 w/w) on top of PEDOT:PSS was carried out with a 25 μm DSP for three layers in a (11 × 11) mm^2 pattern, before annealing at T = 90 °C for 10 min. For the bottom electrode (part B), a combination of AZO and Ag NWs was employed on a second TT. A layer of AZO was first printed on the tattoo paper (10 × 15) mm^2. After applying a Parafilm mask of the same size, 45 μL of Ag NWs was deposited via drop-casting. This was followed by removal of the mask and annealing at T = 120 °C for 2 min followed before another Parafilm mask (same size) was applied. Then again, 45 μL of Ag NWs was drop-cast and the sample was annealed at T = 120 °C for 3 min. Also, a contacting area for the PEDOT:PSS electrode was done in the same manner but with a smaller area. On top of the Ag NWs, five layers of AZO (DSP: 25 μm) were printed on an area of (11 × 11) mm^2 and annealed at 120 °C for 10 min.

https://doi.org/10.1021/acsaelm.1c00249
ACS Appl. Electron. Mater. 2021, 3, 2652−2660

Samples were stored with protection from direct sunlight without other precaution steps.

Characterization. Samples of TT to be used for AFM and Stylus profilometry characterization were cut with scissors and floated on distilled water (T = 30 °C) to allow for detachment of the transferable EC layer. The latter was then recollected onto Si wafers, whereas for UV/vis measurements, similar samples were recollected onto glass microscope slide coverslips.

AFM (topography, roughness) measurements were performed with an easyScan 2 from Nanosurf operating in tapping mode (probes: PPP-NCLR-10 by Nanosensors; resonance frequency: 146−236 kHz; force constant: 21−98 Nm^{-1}) on an area of (10 × 10) μm^2 at four positions per sample (three samples in total). AFM topography images were then further analyzed with Gwyddion software, mainly for leveling, correcting artefacts, and estimating roughness R_a.

Profilometry measurements were carried out with an AlphaStep D-500 stylus profilometer from KLA Tencor, which was placed on an anti-vibration plate from Halcyonics (Micro 40) and used for estimation of thickness t of all materials. To characterize the EC transferable layer from TT, three samples were measured, each at four positions. Scratches were made with tweezers to measure the thickness across a step. The same procedure was applied to estimate the thickness of deposited films, and reference samples were prepared by deposition on glass.

UV/vis spectrophotometry measurements (transmittance) were done with a Shimadzu UV-1800 in a wavelength range of (380−900) nm. Therefore, the examined samples were collected or mounted onto glass slides.

The NIR spectrum was obtained with an ARCOptix FT-NIR Rocket FTNIR-L1-025-2TE-8 spectrometer with a light source from an Ocean Optics HL-2000-HP-FHSA from 900 to 2500 nm. Further components in the setup are an aspheric condenser lens, a Reflection Probe Fiber Bundle ZrF4 of 200 μm core diameter (fiber from the light source), and Thorlabs RP23 200 μm (fiber to the spectrometer), with the aperture set to the spot size of the light beam. Five layers of EC were collected onto a glass slide to obtain better signals.

The four-point measurements were carried out with a custom four-point setup connected to a Keithley 2620B multifunction source meter to determine the sheet resistance of deposited materials. The tips of the four-point probe are linearly arranged with a spacing of 1.5 mm. A current of few milliamperes was used for the measurements of (10 × 10) mm^2 samples and varied slightly depending on the sample.

I/V-characteristic measurements were performed with a custom-made apparatus system with a LED (CREE XLamp: CMA3090-0000-000R0U0A40G), a multimeter DMM 4040 from Tektronix, and an ISO-Tech power supply (IPS 2303S). The illuminance was measured with a MK350 LED meter from UPRtek to be (75 700 ± 300) lx. Measurements of the curve followed the same procedure; at zero bias, the measurements were done without the power supply; after connecting, the voltage increased. After each change of voltage, 30 s were waited before recording 100 data points for statistical means. Before measuring the other direction, the sample was short-circuited to get rid of any possible accumulated charge. The dark condition was measured before the illuminated one.

■ ASSOCIATED CONTENT

Supporting Information

The Supporting Information is available free of charge at https://pubs.acs.org/doi/10.1021/acsaelm.1c00249.

Optical and AFM images of TT; UV/vis spectra of electrodes; printing parameters for PEDOT:PSS; transfer of OPD onto a leaf; NIR spectra of EC; I/V curve of PEDOT:PSS/P3HT:ICBA(1:1 w/w)/Al in the logarithmic scale; I/V curve of a new OPD; printing of a P3P4T:PyC60 layer; UV/vis spectra of BHJ materials; SEM image of Ag NWs on TT; I/V curve of the PEDOT:PSS/P3P4T:PyC60(1:1 w/w)/AZO electrode in the logarithmic scale; and sheet resistance for electrodes (PDF)

■ AUTHOR INFORMATION

Corresponding Author

Francesco Greco − *Institute of Solid State Physics, Graz University of Technology, 8010 Graz, Austria;* orcid.org/0000-0003-2899-8389; Email: francesco.greco@tugraz.at

Authors

Bernhard Burtscher − *Institute of Solid State Physics, Graz University of Technology, 8010 Graz, Austria*

Guenther Leising − *Institute of Solid State Physics, Graz University of Technology, 8010 Graz, Austria*

Complete contact information is available at: https://pubs.acs.org/10.1021/acsaelm.1c00249

Author Contributions

All authors have given approval to the final version of the manuscript.

Notes

The authors declare no competing financial interest.

■ ACKNOWLEDGMENTS

We would like to thank Alexander Dallinger for his help regarding the investigation of printing parameters for PJet 700 and for making the corresponding graph. For their help with the NIR measurement, we would like to thank Stefan Cesnik, Benjamin Lang, and Prof. Alexander Bergmann from the Institute of Electrical Measurement and Sensor Systems, Graz University of Technology.

■ ABBREVIATIONS

AFM, atomic force microscopy; Ag NWs, silver nanowires; AZO, aluminum-doped zinc oxide; BHJ, bulk heterojunction; DSP, drop spacing; EC, ethyl cellulose; ICBA, indene-C60 bisadduct; ID, current without illumination; IL, current with illumination; OPD, organic photodiode; P3HT, poly(3-hexylthiophene); P3P4T, (poly[3-(potassium-4-butanoate)-thiophene-2,5-diyl]); PEDOT:PSS, poly(3,4-ethylenedioxythiophene) doped with polystyrene sulfonate; PyC60, C60 pyrrolidine trisacid ethyl ester; TT, decal transfer temporary tattoo paper

■ REFERENCES

(1) Bandodkar, A. J.; Jia, W.; Wang, J. Tattoo-Based Wearable Electrochemical Devices: A Review. *Electroanalysis* **2015**, *27*, 562−572.

(2) Liu, Y.; Pharr, M.; Salvatore, G. A. Lab-on-Skin: A Review of Flexible and Stretchable Electronics for Wearable Health Monitoring. *ACS Nano* **2017**, *11*, 9614−9635.

(3) Ferrari, L. M.; Sudha, S.; Tarantino, S.; Esposti, R.; Bolzoni, F.; Cavallari, P.; Cipriani, C.; Mattoli, V.; Greco, F. Ultraconformable Temporary Tattoo Electrodes for Electrophysiology. *Adv. Sci.* **2018**, *5*, 1700771.

(4) Yeo, W.-H.; Kim, Y.-S.; Lee, J.; Ameen, A.; Shi, L.; Li, M.; Wang, S.; Ma, R.; Jin, S. H.; Kang, Z.; Huang, Y.; Rogers, J. A. Multifunctional Epidermal Electronics Printed Directly onto the Skin. *Adv. Mater.* **2013**, *25*, 2773−2778.

(5) Ferrari, L. M.; Keller, K.; Burtscher, B.; Greco, F. Temporary Tattoo as Unconventional Substrate for Conformable and Transferable Electronics on Skin and Beyond. *Multifunct. Mater.* **2020**, *3*, 032003.

(6) Bonacchini, G. E.; Bossio, C.; Greco, F.; Mattoli, V.; Kim, Y.-H.; Lanzani, G.; Caironi, M. Tattoo-Paper Transfer as a Versatile Platform for All-Printed Organic Edible Electronics. *Adv. Mater.* **2018**, *30*, 1706091.
(7) Zhao, Y.; Gao, S.; Zhu, J.; Li, J.; Xu, H.; Xu, K.; Cheng, H.; Huang, X. Multifunctional Stretchable Sensors for Continuous Monitoring of Long-Term Leaf Physiology and Microclimate. *ACS Omega* **2019**, *4*, 9522−9530.
(8) Nassar, J. M.; Khan, S. M.; Villalva, D. R.; Nour, M. M.; Almuslem, A. S.; Hussain, M. M. Compliant Plant Wearables for Localized Microclimate and Plant Growth Monitoring. *npj Flexible Electron.* **2018**, *2*, 1−12.
(9) Fu, K. K.; Wang, Z.; Dai, J.; Carter, M.; Hu, L. Transient Electronics: Materials and Devices. *Chem. Mater.* **2016**, *28*, 3527−3539.
(10) Gao, Y.; Zhang, Y.; Wang, X.; Sim, K.; Liu, J.; Chen, J.; Feng, X.; Xu, H.; Yu, C. Moisture-Triggered Physically Transient Electronics. *Sci. Adv.* **2017**, *3*, No. e1701222.
(11) Kang, S.-K.; Yin, L.; Bettinger, C. The Emergence of Transient Electronic Devices. *MRS Bull.* **2020**, *45*, 87−95.
(12) Liu, K.; Tran, H.; Feig, V. R.; Bao, Z. Biodegradable and Stretchable Polymeric Materials for Transient Electronic Devices. *MRS Bull.* **2020**, *45*, 96−102.
(13) Choi, Y.; Koo, J.; Rogers, J. A. Inorganic Materials for Transient Electronics in Biomedical Applications. *MRS Bull.* **2020**, *45*, 103−112.
(14) Han, W. B.; Ko, G.-J.; Shin, J.-W.; Hwang, S.-W. Advanced Manufacturing for Transient Electronics. *MRS Bull.* **2020**, *45*, 113−120.
(15) Ferrari, L. M.; Taccola, S.; Barsotti, J.; Mattoli, V.; Greco, F. Ultraconformable Organic Devices. In *Organic Flexible Electronics*; Elsevier, 2021; pp 437−478.
(16) Heikenfeld, J.; Jajack, A.; Rogers, J.; Gutruf, P.; Tian, L.; Pan, T.; Li, R.; Khine, M.; Kim, J.; Wang, J.; Kim, J. Wearable Sensors: Modalities, Challenges, and Prospects. *Lab Chip* **2018**, *18*, 217−248.
(17) Yang, J. C.; Mun, J.; Kwon, S. Y.; Park, S.; Bao, Z.; Park, S. Electronic Skin: Recent Progress and Future Prospects for Skin-Attachable Devices for Health Monitoring, Robotics, and Prosthetics. *Adv. Mater.* **2019**, *31*, 1904765.
(18) Corbett, B.; Loi, R.; Zhou, W.; Liu, D.; Ma, Z. Transfer Print Techniques for Heterogeneous Integration of Photonic Components. *Prog. Quant. Electron.* **2017**, *52*, 1−17.
(19) Linghu, C.; Zhang, S.; Wang, C.; Song, J. Transfer Printing Techniques for Flexible and Stretchable Inorganic Electronics. *npj Flexible Electron.* **2018**, *2*, 26.
(20) Lai, S.; Zucca, A.; Cosseddu, P.; Greco, F.; Mattoli, V.; Bonfiglio, A. Ultra-Conformable Organic Field-Effect Transistors and Circuits for Epidermal Electronic Applications. *Org. Electron.* **2017**, *46*, 60−67.
(21) Jia, W.; Valdés-Ramírez, G.; Bandodkar, A. J.; Windmiller, J. R.; Wang, J. Epidermal Biofuel Cells: Energy Harvesting from Human Perspiration. *Angew. Chem. Int. Ed.* **2013**, *52*, 7233−7236.
(22) Zucca, A.; Cipriani, C.; Sudha; Tarantino, S.; Ricci, D.; Mattoli, V.; Greco, F. Tattoo Conductive Polymer Nanosheets for Skin-Contact Applications. *Adv. Healthcare Mater.* **2015**, *4*, 983−990.
(23) Ferrari, L. M.; Ismailov, U.; Badier, J.-M.; Greco, F.; Ismailova, E. Conducting Polymer Tattoo Electrodes in Clinical Electro- and Magneto-Encephalography. *npj Flexible Electron.* **2020**, *4*, 1−9.
(24) Piva, N.; Greco, F.; Garbugli, M.; Iacchetti, A.; Mattoli, V.; Caironi, M. Tattoo-Like Transferable Hole Selective Electrodes for Highly Efficient, Solution-Processed Organic Indoor Photovoltaics. *Adv. Electron. Mater.* **2018**, *4*, 1700325.
(25) Barsotti, J.; Rapidis, A. G.; Hirata, I.; Greco, F.; Cacialli, F.; Mattoli, V. Ultrathin, Ultra-Conformable, and Free-Standing Tattooable Organic Light-Emitting Diodes. *Adv. Electron. Mater.* **2021**, *7*, 2001145.
(26) Al-Halhouli, A.; Qitouqa, H.; Alashqar, A.; Abu-Khalaf, J. Inkjet Printing for the Fabrication of Flexible/Stretchable Wearable Electronic Devices and Sensors. *Sens. Rev.* **2018**, *38*, 438−452.
(27) Berchmans, S.; Bandodkar, A. J.; Jia, W.; Ramírez, J.; Meng, Y. S.; Wang, J. An Epidermal Alkaline Rechargeable Ag-Zn Printable Tattoo Battery for Wearable Electronics. *J. Mater. Chem. A* **2014**, *2*, 15788−15795.
(28) Jeerapan, I.; Sempionatto, J. R.; Wang, J. On-Body Bioelectronics: Wearable Biofuel Cells for Bioenergy Harvesting and Self-Powered Biosensing. *Adv. Funct. Mater.* **2019**, *30*, 1906243.
(29) Kim, J.; Gutruf, P.; Chiarelli, A. M.; Heo, S. Y.; Cho, K.; Xie, Z.; Banks, A.; Han, S.; Jang, K. I.; Lee, J. W.; Lee, K. T.; Feng, X.; Huang, Y.; Fabiani, M.; Gratton, G.; Paik, U.; Rogers, J. A. Miniaturized Battery-Free Wireless Systems for Wearable Pulse Oximetry. *Adv. Funct. Mater.* **2017**, *27*, 1604373.
(30) Khan, Y.; Han, D.; Pierre, A.; Ting, J.; Wang, X.; Lochner, C. M.; Bovo, G.; Yaacobi-Gross, N.; Newsome, C.; Wilson, R.; Arias, A. C. A Flexible Organic Reflectance Oximeter Array. *Proc. Natl. Acad. Sci. U.S.A.* **2018**, *115*, E11015−E11024.
(31) Ryu, G.-S.; You, J.; Kostianovskii, V.; Lee, E.-B.; Kim, Y.; Park, C.; Noh, Y.-Y. Flexible and Printed PPG Sensors for Estimation of Drowsiness. *IEEE Trans. Electron Devices* **2018**, *65*, 2997−3004.
(32) Yokota, T.; Zalar, P.; Kaltenbrunner, M.; Jinno, H.; Matsuhisa, N.; Kitanosako, H.; Tachibana, Y.; Yukita, W.; Koizumi, M.; Someya, T. Ultraflexible Organic Photonic Skin. *Sci. Adv.* **2016**, *2*, No. e1501856.
(33) Lim, C.-J.; Kim, J.-H.; Park, J.-W. Highly Flexible and Solution-Processed Organic Photodiodes and Their Application to Optical Luminescent Oxygen Sensors. *Org. Electron.* **2019**, *65*, 100−109.
(34) Yokota, T.; Nakamura, T.; Kato, H.; Mochizuki, M.; Tada, M.; Uchida, M.; Lee, S.; Koizumi, M.; Yukita, W.; Takimoto, A.; Someya, T. A Conformable Imager for Biometric Authentication and Vital Sign Measurement. *Nat. Electron* **2020**, *3*, 113−121.
(35) Lamprecht, B.; Thünauer, R.; Ostermann, M.; Jakopic, G.; Leising, G. Organic Photodiodes on Newspaper. *Phys. Status Solidi A* **2005**, *202*, R50−R52.
(36) Rafique, S.; Abdullah, S. M.; Sulaiman, K.; Iwamoto, M. Fundamentals of Bulk Heterojunction Organic Solar Cells: An Overview of Stability/Degradation Issues and Strategies for Improvement. *Renew. Sustain. Energy Rev.* **2018**, *84*, 43−53.
(37) Takata, Y.; Hidaka, S.; Kohno, M. Wettability Improvement by Plasma Irradiation and Its Applications to Phase-Change Phenomena. *Heat Transfer Eng.* **2009**, *30*, 549−555.
(38) Burtscher, B.; Thesis, M. S. *Inkjet Printed Organic Photodiode on an Ultrathin, Commercial, Conformal and Transferrable Polymer Substrate*; Graz University of Technology, 2019.
(39) Dallinger, A.; Keller, K.; Fitzek, H.; Greco, F. Stretchable and Skin-Conformable Conductors Based on Polyurethane/Laser-Induced Graphene. *ACS Appl. Mater. Interfaces* **2020**, *12*, 19855.
(40) Wasilewska, K.; Winnicka, K. Ethylcellulose-A Pharmaceutical Excipient with Multidirectional Application in Drug Dosage Forms Development. *Materials* **2019**, *12*, 3386.
(41) Nawrocki, R. A. Super- and Ultrathin Organic Field-Effect Transistors: from Flexibility to Super- and Ultraflexibility. *Adv. Funct. Mater.* **2019**, *29*, 1906908.
(42) Lövenich, W. PEDOT-Properties and Applications. *Polym. Sci., Ser. C* **2014**, *56*, 135−143.
(43) Heng, P. W. S.; Chan, L. W.; Ong, K. T. Influence of Storage Conditions and Type of Plasticizers on Ethylcellulose and Acrylate Films Formed from Aqueous Dispersions. *J. Pharm. Pharm. Sci.* **2003**, *6*, 334.
(44) Wypych, G. EC Ethyl Cellulose. In *Handbook of Polymers*; Elsevier, 2016; pp 102−104.
(45) Guo, X.; Zhang, M.; Cui, C.; Hou, J.; Li, Y. Efficient Polymer Solar Cells Based on Poly(3-Hexylthiophene) and Indene-C60 Bisadduct Fabricated with Non-Halogenated Solvents. *ACS Appl. Mater. Interfaces* **2014**, *6*, 8190−8198.
(46) Kadem, B.; Fakher Alfahed, R. K.; Al-Asadi, A. S.; Badran, H. A. Morphological, Structural, Optical, and Photovoltaic Cell of Copolymer P3HT: ICBA and P3HT:PCBM. *Optik* **2020**, *204*, 164153.

https://doi.org/10.1021/acsaelm.1c00249
ACS Appl. Electron. Mater. 2021, 3, 2652−2660

(47) Yan, X.; Ma, J.; Xu, H.; Wang, C.; Liu, Y. Fabrication of Silver Nanowires and Metal Oxide Composite Transparent Electrodes and Their Application in UV Light-Emitting Diodes. *J. Phys. D: Appl. Phys.* **2016**, *49*, 325103.
(48) Lai, H. L.; Pitt, K.; Craig, D. Q. M. Characterisation of the Thermal Properties of Ethylcellulose Using Differential Scanning and Quasi-Isothermal Calorimetric Approaches. *Int. J. Pharm.* **2010**, *386*, 178−184.
(49) Sakellariou, P.; Rowe, R. C.; White, E. F. T. The Thermomechanical Properties and Glass Transition Temperatures of Some Cellulose Derivatives Used in Film Coating. *Int. J. Pharm.* **1985**, *27*, 267−277.
(50) Thalluri, G. K. V. V.; Bolsée, J.-C.; Gadisa, A.; Parchine, M.; Boonen, T.; D'Haen, J.; Boyukbayram, A. E.; Vandenbergh, J.; Cleij, T. J.; Lutsen, L.; Vanderzande, D.; Manca, J. Opto-Electrical and Morphological Characterization of Water Soluble Conjugated Polymers for Eco-Friendly Hybrid Solar Cells. *Sol. Energy Mater. Sol. Cells* **2011**, *95*, 3262−3268.
(51) McKeen, L. W. Environmentally Friendly Polymers. In *Plastics Design Library*, 4th ed.; William Andrew Publishing, 2017; pp 305−323.

https://doi.org/10.1021/acsaelm.1c00249
ACS Appl. Electron. Mater. 2021, 3, 2652−2660